

PREDICTION OF FORMATION OF ORIENTED LAKES

Takaaki Uda¹, Masumi Serizawa², Toshiro San-nami² and Shiho Miyahara²

In vast areas of the Arctic Coastal Plain, oriented lakes, groups of lake basins with a common long-axis orientation, can be found. Numerical simulation using the BG model (a three-dimensional model for predicting beach changes based on Bagnold's concept) was carried out, and the characteristic of oriented lakes that the direction of their principal axis is perpendicular to that of the principal axis of the probability distribution of occurrence of wind direction was successfully explained. The predicted results and the examples given by Seppälä (2004) were in good agreement.

Keywords: Oriented lakes; wind waves; lakeshore changes; segmentation; BG model

INTRODUCTION

In a shallow water body, beach changes may take place owing to wind waves. In a narrow water body with a large aspect ratio, the wave incidence angle relative to the normal to the shoreline may exceed 45° and the shoreline may become unstable to form cusped forelands (Zenkovich, 1967; Ashton and Murray, 2006; Ashton et al., 2009). Ashton et al. (2009) developed a model for predicting lakeshore changes on the basis of longshore sand transport formula, and predicted that the forelands formed along the shoreline connect with each other, resulting in the segmentation of the water body into smaller rounded lakes. Uda et al. (2012) predicted the three-dimensional (3-D) segmentation of a shallow rectangular water body using the BG model (a 3-D model for predicting beach changes based on Bagnold's concept) proposed by Serizawa et al. (2006). Furthermore, Uda et al. (2013) studied the emergence and merge of small lakes and their segmentation using the same model. In these calculations, the shape of the lakes formed after the segmentation was a complete circle. In vast areas of the Arctic Coastal Plain, oriented lakes, as shown in Fig. 1, can be found, and they are groups of lake basins with a common long-axis orientation (Seppälä, 2004). The direction of the principal axis is normal to the wind direction in summer (Seppälä, 2004). Oriented lakes in permafrost regions were originally thermokarst features (Harry & Fench, 1983). The shape of oriented lakes in North America is often elliptical with their long axis generally aligned in the N-NW direction, perpendicular to the prevailing summer winds. The initial cause of the formation of a thaw lake or depression may be the random melting of ground ice or subsidence of the ground followed by the accumulation of water in the depression. Mackay (1963) developed a mathematical model that relates the lake shape with the resultant wind vectors and the square of the velocity, and attempted to analyze the equilibrium forms of lakes that might be produced by winds of today. However, he emphasized that the precise mechanism of the lake orientation remains unexplained. In this study, the formative mechanism of oriented lakes was investigated using the BG model.

EXAMPLES OF ORIENTED LAKES

In the Arctic Coastal Plain, typical examples of oriented lakes can be found from the satellite images, in addition to the geomorphological classification of oriented lakes, as shown in Fig. 1, originally drawn by Seppälä (2004). Figure 2 shows the satellite image of the coastal lowland at a location ($69^\circ 13' 41.66''\text{N}$, $160^\circ 01' 39.84''\text{E}$) with an elevation of 8 m above mean sea level, facing the East Siberian Sea and expanding west of the Kolyma River in east Siberia in Russia. In this area, many lakes have been formed and the Kolyma River flows into the East Siberian Sea. Three oriented lakes with the principal axis of the northwest-southeast direction can be seen 20 km west of the Kolyma River, and each lake is separated by a slender sand bar. Seaward of these lakes, many ridges extend in parallel to the shoreline, and the principal axis of these oriented lakes is in parallel to the shoreline. From these characteristics, it is inferred that oriented lakes of this shape could develop because the strength of the sea breeze is larger than that of the wind blowing from the other direction. Furthermore, a number of small lakes can be seen inland of these oriented lakes, and the shape of those lakes is also distorted in the south-north direction with a principal axis of the east-west direction.

The second example is the development of oriented lakes west of Point Barrow ($70^\circ 55' 32.54''\text{N}$, $157^\circ 27' 37.11''\text{W}$) in north Alaska separating the Chukchi and Beaufort Seas. Figure 3 shows the

¹ Public Works Research Center, 1-6-4 Taito, Taito, Tokyo 110-0016, Japan

² Coastal Engineering Laboratory Co., Ltd., 1-22-301 Wakaba, Shinjuku, Tokyo 160-0011, Japan

satellite image of the area. Schematic figure of oriented lakes, as shown in Fig. 1 (Seppälä, 2004), was drawn, focusing on the area east of Point Barrow, but in this study, the area west of Point Barrow was selected to investigate the relationship between the direction of incident waves and the development of oriented lakes. In Fig. 3, sand spits and hooked shoreline, which were assumed to have developed owing to the shoreline instability (Ashton et al., 2001; Falqués, 2008; Serizawa et al., 2012), run in the southwest-northeast direction. Figure 4 shows the enlarged satellite image of the rectangular area in Fig. 3. A number of oriented lakes can be found with the direction of the principal axis of approximately $N7^{\circ}W$. The direction normal to this axis is $N97^{\circ}W$, and wind of this direction is assumed to have a primary effect to the formation of oriented lakes. This wind direction makes a large angle of 82° to the direction of $N15^{\circ}W$ normal to the shoreline of the sand spit located at the left end in Fig. 4. Considering that wind waves are generated by wind from this direction, the shoreline instability could occur because of a large angle of wave incidence. Thus, in this case, the development of oriented lakes owing to the intensive prevailing wind and the occurrence of the shoreline instability correspond well.

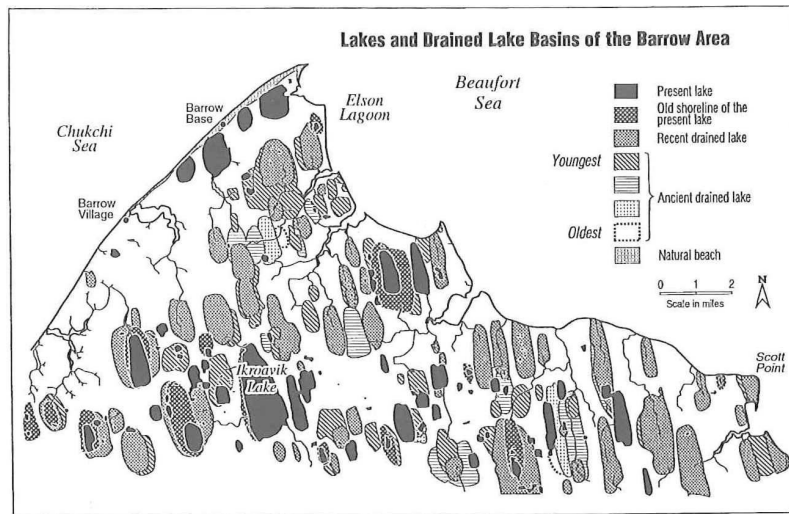


Figure 1. Oriented lakes (Seppälä, 2004).

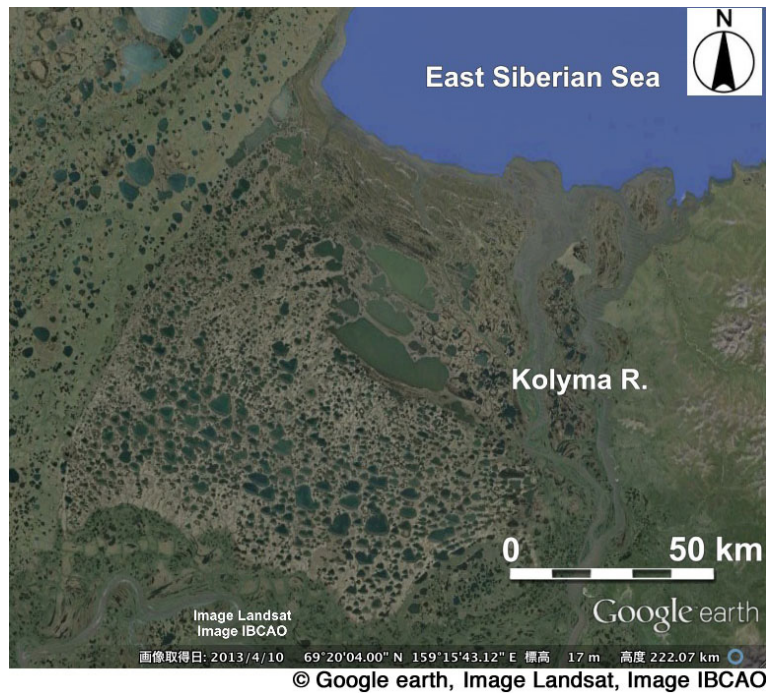


Figure 2. Example of oriented lakes in east Siberia.



Figure 3. Oriented lakes west of Point Barrow in Alaska separating Chukuchi Sea and Beaufort Sea.



Figure 4. Enlarged satellite image of rectangular area shown in Fig. 3.

NUMERICAL SIMULATION USING THE BG MODEL

The fundamental equations used in this study are the same as those proposed by Uda et al. (2012; 2013). For the sand transport equation, Eq. (1), which is expressed using the wave energy at the breaking point, was used, similar to the BG model proposed by Serizawa et al. (2006). The variables in Eq. (1) are given by Eqs. (2) - (9).

$$\bar{q} = C_0 \frac{K_s P}{\tan \beta_c} \left\{ \tan \beta_c \bar{e}_w - |\cos \alpha| \sqrt{\nabla Z} \right\} \quad (-h_c \leq Z \leq h_R) \quad (1)$$

$$P = \varepsilon(Z) (EC_g)_b \tan \beta_w \quad (P \geq 0) \quad (2)$$

$$\tan \beta_w = dZ / dx_w \quad (\tan \beta_w \geq 0) \quad (3)$$

$$\int_{-h_c}^{h_R} \varepsilon(Z) dZ = 1 \quad (4)$$

$$\varepsilon(Z) = \frac{1}{h_c + h_R} \quad (-h_c \leq Z \leq h_R) \quad (5)$$

$$(EC_g)_b = C_1 (H_b)^{\frac{5}{2}} \approx C_1 (H_{1/3})^{\frac{5}{2}} \quad (6a)$$

$$C_1 = \frac{\rho_s g}{k_1} \sqrt{g/\gamma} \quad (k_1 = (4.004)^2, \gamma = 0.8) \quad (6b)$$

$$F^{(i+1)} = F^{(i)} + r \Delta x_w \quad (7a)$$

$$r = \begin{cases} 1 & (Z \leq 0) \\ 0 & (Z > 0) \end{cases} \quad (7b)$$

$$F^{(i)} = 0 \quad (\text{if } Z \geq 0 \text{ and } dZ/dx_w \leq 0) \quad (8)$$

$$\begin{aligned} H_{1/3} &= f(F, U) \\ &= 0.30 \left\{ 1 - \left[1 + 0.004 (gF/U^2)^{1/2} \right]^2 \right\} (U^2/g) \end{aligned} \quad (9)$$

$$\partial Z / \partial t + \nabla \cdot \vec{q} = 0 \quad (10)$$

Here, $\vec{q} = (q_x, q_y)$ is the net sand transport flux, $Z(x, y, t)$ is the seabed elevation with reference to the still water level ($Z = 0$), $\vec{\nabla} Z = (\partial Z / \partial x, \partial Z / \partial y)$ is the seabed slope vector, \vec{e}_w is the unit vector of wave direction, α is the angle between the wave direction and the direction normal to the contour line, x_w is the coordinate along the direction of wave propagation, $\tan \beta_w$ is the seabed slope measured along the direction of wave propagation, $\tan \beta_c$ is the equilibrium slope of sand, and K_s is the longshore and cross-shore sand transport coefficient. C_0 is the coefficient transforming the immersed weight expression to the volumetric expression ($C_0 = 1 / \{(\rho_s - \rho)g(1 - p)\}$; ρ is the sea water density, ρ_s is the specific gravity of sand, p is the porosity of sand, and g is the acceleration due to gravity), h_c is the depth of closure, and h_R is the berm height. $\varepsilon(Z)$ is the depth distribution of sand transport and is defined using Eq. (4), and in this study, a uniform distribution was employed (Eq. (5)). $(EC_g)_b$ is the wave energy flux at the breaking point, H_b is the breaker height, $H_{1/3}$ is the significant wave height calculated by the S-M-B methods, and γ is the ratio of the breaker height relative to the water depth. In addition, $k_1 = (4.004)^2$ in Eq. (6b) is a constant in the relationship between the wave energy E and the significant wave height when the probability of the wave height of irregular waves is assumed to be given by the Rayleigh distribution (Horikawa, 1988). F is the local fetch, U is the wind velocity. The index i in Eq. (7a) is the mesh number along the x_w -axis.

In the calculation, the local beach slope measured along the wave ray was used for the beach slope in Eq. (2), as shown in Eq. (3). Prior to the calculation of beach changes, the significant wave height at a point was calculated by the S-M-B methods (Komar, 1998) given a local fetch F at a point and wind velocity U . In this calculation, a fixed coordinate system of (x, y) was adopted for the calculation of beach changes with the calculation domain of rectangular shape of ABCD, as shown in Fig. 5, whereas another coordinate system of (x_w, y_w) was set corresponding to the wave direction, and the wave height was calculated in the rectangular domain of A'B'C'D' including the domain ABCD.

Neglecting the wave refraction effect, waves are assumed to propagate in the same direction as the wind. The x_w -axis was subdivided by the mesh intervals of Δx_w . The fetch F was added from upwind to downwind along the x_w -axis using Eq. (7). When a grid point was located on land and the downslope condition of $dZ/dx_w \leq 0$ was satisfied, the local fetch was reset as $F = 0$ (Eq. 8). When the grid point

was again located in the lake, F was recalculated. Then, the significant wave height was calculated with Wilson's (1965) equation (Eq. (9)) using the wind fetch F and wind velocity U (Goda, 2003), and this wave height was assumed to be equal to the breaker height (Eq. 6(a)). Simultaneously, the wave power P (Eq. (2)) was calculated and assigned to each grid point on the coordinates of (x_w, y_w) . The wave power P at each grid point in the calculation of beach changes was interpolated from this distribution of the wave power P .

In this study, the wind direction at each step in the calculation of beach changes was selected to be a value determined by random numbers so as to satisfy the probability distribution function of occurrence of wind direction, although wind velocity was assumed to be constant. Every step of the calculation of beach changes, the wind direction was reset by random numbers, and the distribution of P value was recalculated. Finally, the sand transport and continuity equations of Eqs. (1) and (10) were solved on the x - y plane by the explicit finite-difference method using the staggered mesh scheme. With regard to Eq. (7b), a reduction factor was introduced depending on the water depth in a zone with the depth shallower than h_c in the previous papers (Uda et al., 2012; 2013). However, a reduction factor was not introduced in the present study, because the water depth is mostly shallower than h_c in the present study, and wind fetch should be underestimated upon introducing such a reduction factor.

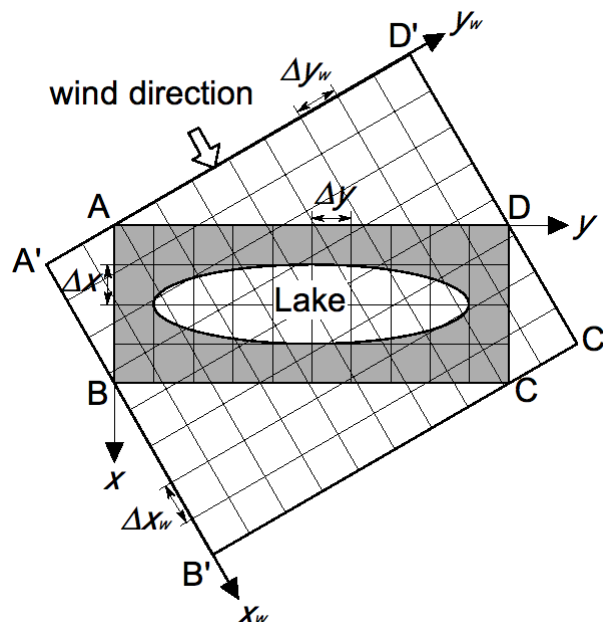


Figure 5. Two coordinate systems.

Calculation Conditions

A shallow lake with a flat sandy bed of water depths of $Z = -0.5, -0.75$ and -1.0 m was assumed as the initial topography, as shown in Fig. 6, to investigate the effect of the difference in initial water depth (or the thickness of sand layer above a solid bed with the water depth of -3 m) to the development of the oriented lakes. The thickness of sand layer increases in the order of Cases 1, 2 and 3, as 2, 2.25 and 2.5 m, resulting in the increase in volume of movable sand under waves. The calculation domain was a rectangle with 2.4 km length and 1 km width. The boundary of the lake was given by a solid vertical wall.

At the initial stage, random noise of $\Delta Z = 0.1$ m was added to the lakebed. The berm height and depth of closure were assumed to be 1 m and 3 m, respectively. The water depth of the flat shallow lake in each case was shallower than the depth of closure, so that sand deposited on the flat bed at the initial stage could be quickly redistributed by wave action, leading to the formation of a sloping beach. The wind velocity was assumed to be 20 m/s, and an asymmetric probability distribution for the occurrence of wind direction with an aspect ratio of 4 was assumed, such that the principal axis of the probability of occurrence of wind direction was at an angle of 45° to the x -axis (Fig. 7), although the wind was assumed to blow uniformly from all directions between 0° and 360° in Uda et al. (2013), i.e., a symmetric circular distribution was assumed. Wind velocity of 20 m/s employed in this study is the one

which generates approximately 0.7 m of significant wave height, given the wind fetch along the diagonal in the initial lake as 2.6 km. The calculation domain was discretized by 20 m meshes, Δt was selected to be 10 hr and the calculation was carried out for up to 10^5 steps (Table. 1).

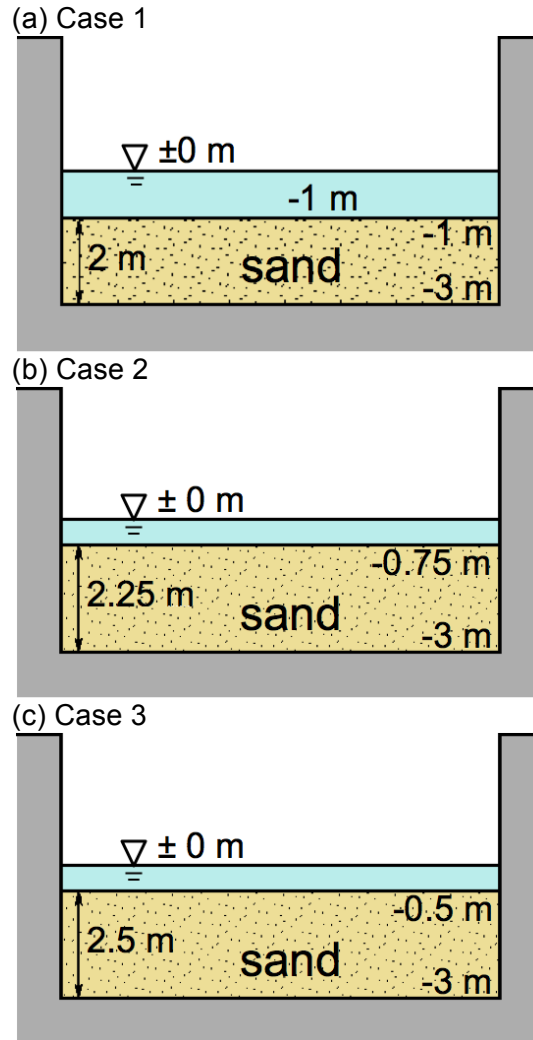


Figure 6. Initial lakebed composed of sand.

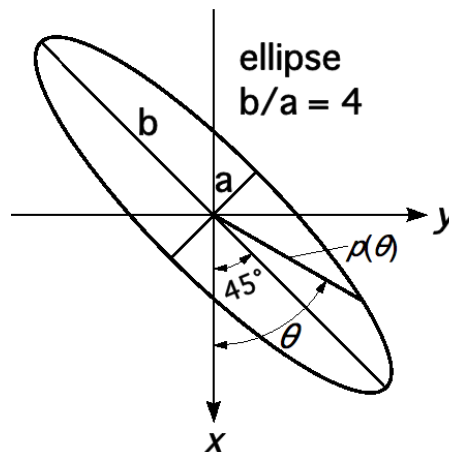


Figure 7. Probability distribution of occurrence of wind direction.

Table 1. Calculation conditions.	
Wind velocity	20 m/s
Berm height h_R	1 m
Depth of closure h_c	3 m
Equilibrium slope $\tan\beta_c$	1/20
Coefficients of sand transport	longshore and cross-shore sand transport coefficient $K_s = 0.2$
Mesh size	$\Delta x = \Delta y = 20$ m
Time intervals	$\Delta t = 10$ hr
Duration of calculation	10^6 hr (10^5 step)
Boundary conditions	Shoreward and landward ends $q_x = 0$ Right and left boundaries $q_y = 0$

RESULTS

Planar Change in Oriented Lakes

The calculation results in Case 1 are shown in Fig. 8. When wind blew obliquely to the shallow body of water with a 1 m depth, a number of slender small lakes had emerged after 2×10^3 steps via the mechanism proposed by Uda et al. (2013). Up to 4×10^3 steps, these slender small lakes had merged into larger lakes and the width of the lakes increased. After 6×10^3 steps, small lakes had further merged into larger lakes, although the characteristics of the oriented lakes were unclear at this stage. After 2×10^4 steps, two large lakes as an original form of the oriented lakes had developed owing to the mergence of small lakes, and after 3×10^4 steps, oriented lakes of almost elliptic shape were formed. Finally, after 1×10^5 steps, oriented lakes of completely elliptic shape were formed. The direction of the principal axis of the oriented lakes became normal to the direction of the principal axis of the probability distribution of occurrence of wind, as shown in Fig. 7.

Similarly, the results of Case 2 with a 0.75 m depth are shown in Fig. 9. After 2×10^3 steps, a number of small lakes had randomly emerged. After 4×10^3 steps, small lakes had merged into larger lakes, while reducing the number of lakes. After 6×10^3 steps, the number of small lakes was further reduced with the mergence of small lakes. After 2×10^4 steps, oriented lakes of almost elliptic shape were formed, and finally oriented lakes of completely elliptic shape were formed after 1×10^5 steps. Comparing the results after 1×10^5 steps of Cases 1 and 2, the number of oriented lakes increased and the size of the oriented lakes reduced in Case 2.

Figure 10 shows the same results of Case 3 with a 0.5 m depth shallower than the other cases. After 2×10^3 steps, a number of small lakes of irregular shape had randomly emerged. After 4×10^3 steps, the small lakes similar to the oriented lakes had formed owing to the mergence of the small lakes, and then they merged into larger lakes by 6×10^3 steps. It was apparent that oriented lakes were gradually being formed owing to the mergence of small lakes after 1×10^4 steps, and after 2×10^4 the size of the small lakes had increased with the further mergence of lakes. After 5×10^4 steps, many oriented lakes had formed. With time, the number of lakes decreased and their size increased as a result of their mergence. Finally, after 1×10^5 steps, highly oriented lakes with an elliptical shape had formed.

Although the volume of movable sand in the calculation domain increased in the order of Cases 1, 2 and 3, the size of the oriented lakes decreased in this order together with the increase in number of oriented lakes. Because the size of the water body, where sand movement occurs, reduced in the order of Cases 1, 2 and 3, the mergence of small lakes became difficult to occur. Thus, the oriented lakes quickly reached a stable shape without the development of the oriented lakes of sufficiently large size. In addition, the coexistence of the oriented lakes of various scales as seen in the results between 1×10^4 and 1×10^5 steps is found in the examples of the oriented lakes, as shown in Figs. 1, 2 and 4.

The reason that the direction of the principal axis of oriented lakes becomes normal to the direction of principal axis in the elliptic probability distribution of occurrence of wind direction is considered as follows. Although the wind fetch along the minor axis of oriented lakes is short and thus weaker wind waves are generated, the probability of occurrence of wind direction is large. In contrast, although the wind fetch is longer along the principal axis of the oriented lakes, causing stronger wind waves, the probability of occurrence is low. Taking these features into account, the action along the principal and minor axes may balance each other, and the oriented lakes of elliptic shape could be formed.

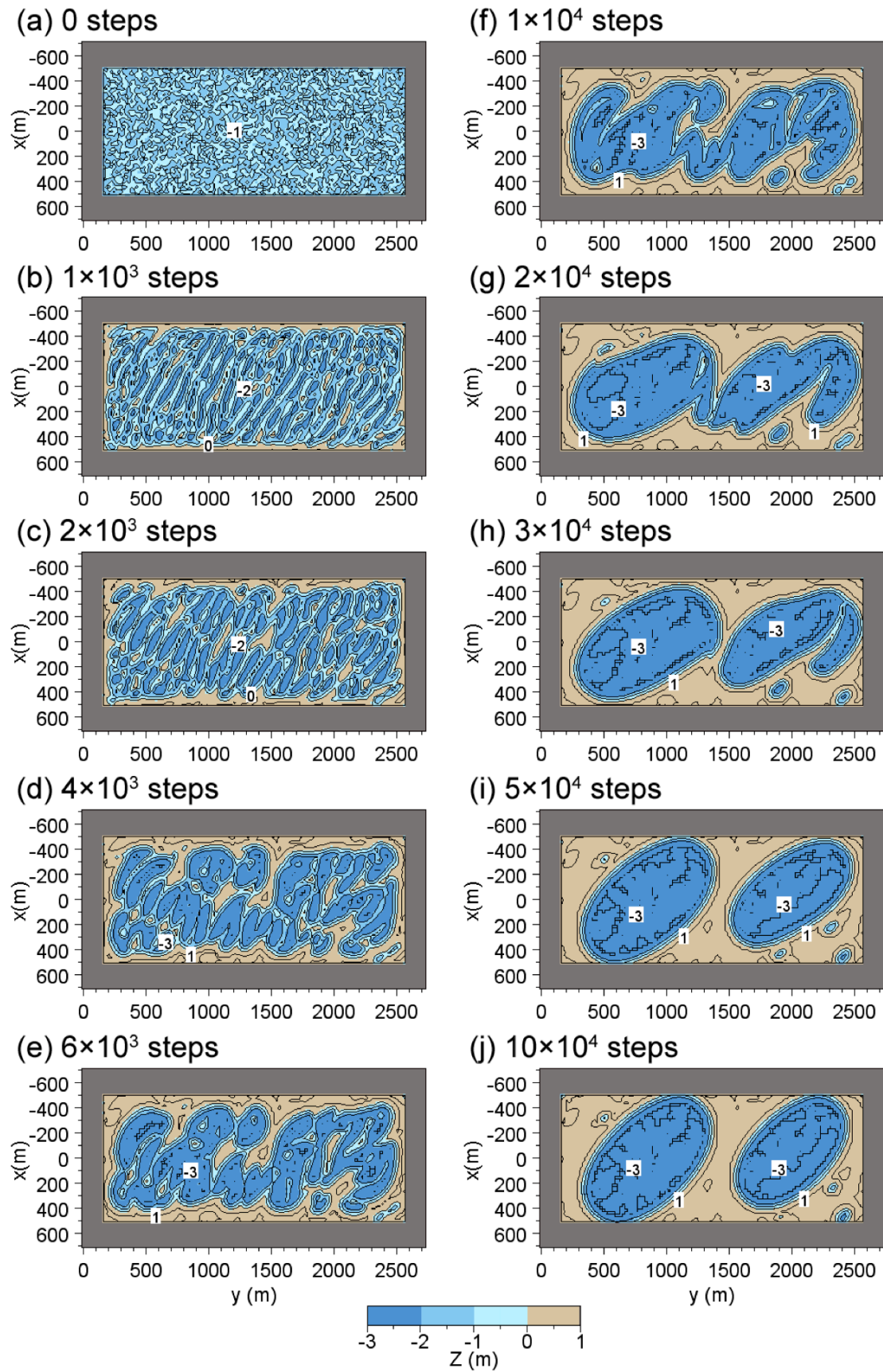


Figure 8. Prediction results of oriented lakes (Case 1).

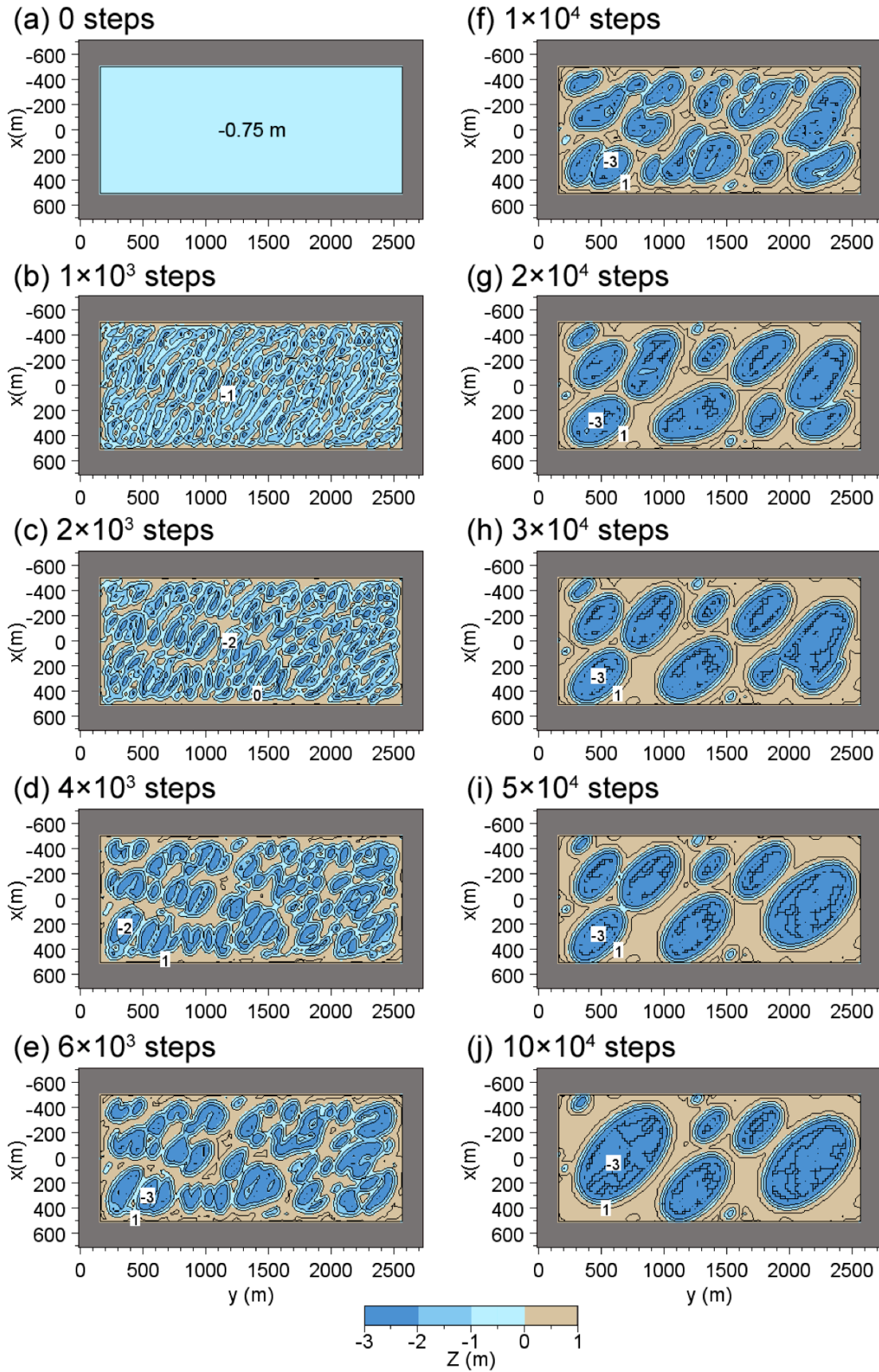


Figure 9. Prediction results of oriented lakes (Case 2).

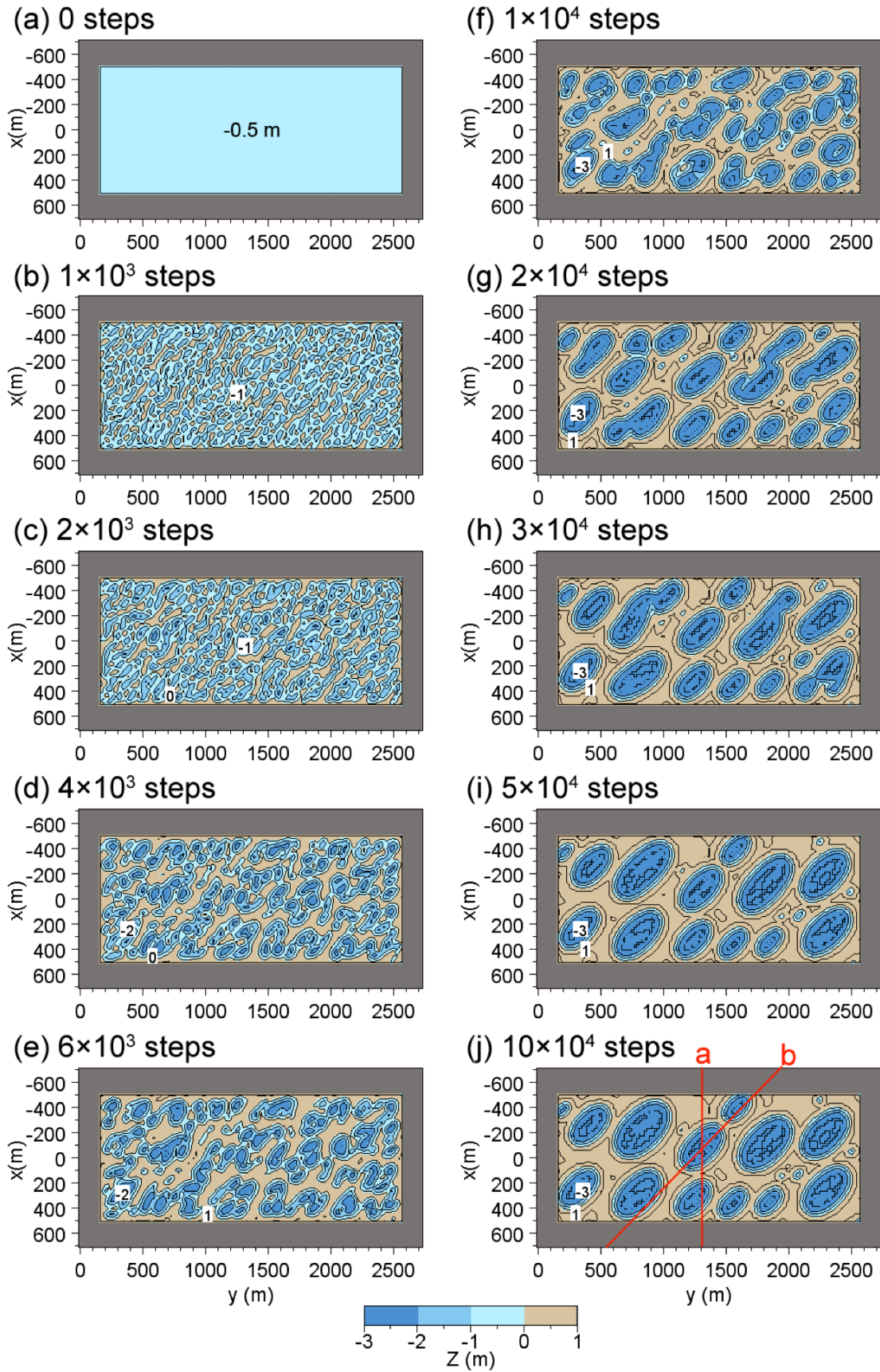


Figure 10. Prediction results of oriented lakes (Case 3).

Profile Changes

In the planar distribution after 1×10^5 steps in Case 3, when oriented lakes have sufficiently developed, as shown in Fig. 10, the cross-sections *a* and *b* traversing oriented lakes along the *x*-axis and the principal axis of oriented lakes were selected, and the profile changes along these cross-sections were investigated (Fig. 11). Along cross section *a*, irregular perturbation given on the flat lakebed with an initial water depth of 0.5 m increased in scale with time, and many small lakes with various water depths were formed. Then these small lakes merged each other to form larger lakes. After 1×10^5 steps, large lakes with a flat bottom of 3 m depth was formed. Similarly, oriented lakes developed along cross section *b* in the same manner.

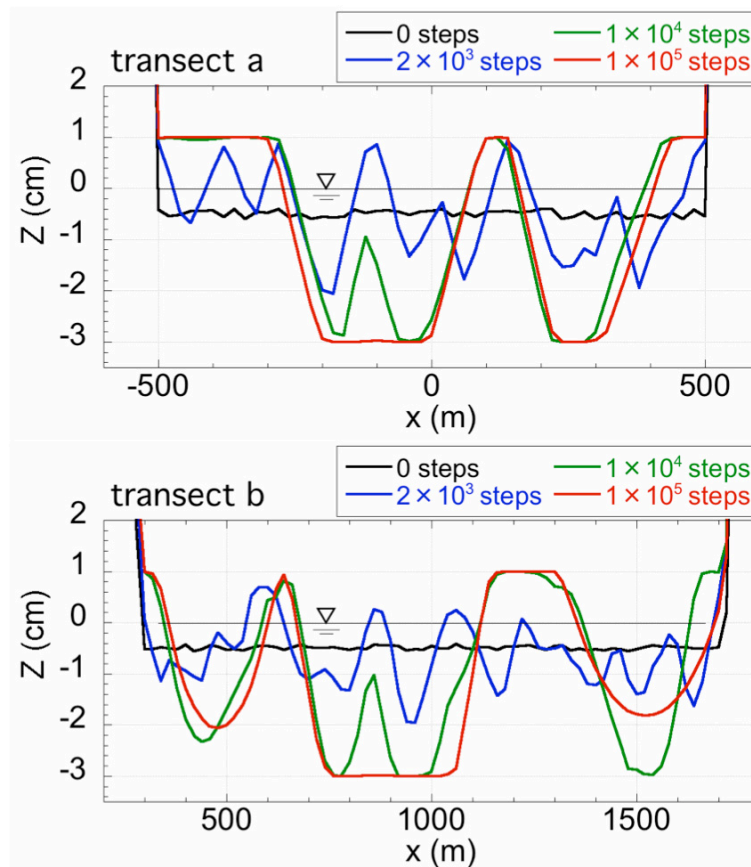


Figure 11. Profile changes across transects a and b in Case 3.

CONCLUSIONS

In the numerical simulation of the formation of a lake carried out by Uda et al. (2012; 2013), in which wind was assumed to blow uniformly from all directions between 0° and 360° , i.e., a symmetric circular distribution was assumed, a lake with a highly circular shape was formed (Uda et al., 2013). In this study, the shape of the lakes became elliptical because of asymmetric probability distribution of occurrence of wind direction. The characteristic of oriented lakes that the direction of their principal axis is perpendicular to the principal axis of probability distribution of occurrence of wind direction was successfully explained by the BG model. The predicted results and the examples given by Seppälä (2004) were in good agreement. Ashton et al. (2009) carried out the calculation of the segmentation of a rectangular lake given the symmetrical distribution (uniform in entire direction) of the probability of occurrence of waves (wind direction), and they concluded that when the probability distribution is assumed to be asymmetrical, elliptic lakes were formed. The results of the present study confirmed this result. Because the BG model is a 3-D model for predicting beach changes, the process of the 3-D lakeshore changes can be calculated even under the initial condition that sand is distributed only on the lakebed, whereas the lakeshore shoreline exists from the beginning because of the tracking of the shoreline change on the *x*-*y* meshes as in Ashton et al. (2009).

REFERENCES

- Ashton, A., Murray, A. B., and Arnault, O. 2001. Formation of coastline features by large-scale instabilities induced by high angle waves, *Nature*, Vol. 414, pp. 296-300.
- Ashton, A., and Murray, A. B. 2006. High-angle wave instability and emergent shoreline shapes: 1. Modeling of sand waves, flying spits, and capes, *J. Geophys. Res.*, Vol. 111, F04011, doi: 10.1029/2005JF000422.
- Ashton, A., Murray, A. B., Littlewood, R., Lewis, D. A., and Hong, P. 2009. Fetch limited self-organization of elongate water bodies, *Geology*, Vol. 37, 187-190.
- Falqués, A., van den Berg, N., and Calvete, D. 2008. The role of cross-shore profile dynamics on shoreline instability due to high-angle waves, *Proc. 31st ICCE*, pp. 1826-1838.
- Goda, Y. 2003. Revisiting Wilson's formulas for simplified wind-wave prediction, *J. Waterway, Port, Coastal and Ocean Engineering*, Vol. 129, No. 2, pp. 93-95.
- Harry, D. G., and French, H. M. 1983. The orientation and evolution of thaw lakes, southwest Banks Island, *Canadian Arctic, in Proceedings, Fourth International Conference on Permafrost*, pp. 456-461, Natl. Acad. of Sci., Washington, D. C.
- Horikawa, K. ed. 1988. *Nearshore Dynamics and Coastal Processes*, University of Tokyo Press, Tokyo, 522 pp.
- Komar, P. D. 1998. *Beach Processes and Sedimentation*, Prentice Hall International, London, 544 p.
- Mackay, J. R. 1963. *The Mackenzie Delta Area*, N.W.T. Geographical Branch, Mines and Technical Surveys, Ottawa, Memoir 8, 202 p.
- Seppälä, M. 2004. *Wind as a Geomorphic Agent in Cold Climates*, Cambridge University Press, p. 358.
- Serizawa, M., Uda, T., San-nami, T., and Furuike, K. 2006. Three-dimensional model for predicting beach changes based on Bagnold's concept, *Proc. 30th ICCE*, pp. 3155-3167.
- Serizawa, M., Uda, T., and Miyahara, S. 2012. Prediction of development of sand spits and cusped forelands with rhythmic shapes caused by shoreline instability using BG model, *Proc. 33rd ICCE*, sediment.35, pp. 1-11.
- Uda, T., Serizawa, M., and Miyahara, S. 2012. Numerical simulation of three-dimensional segmentation of elongated water body using BG model, *Proc. 33rd ICCE*, sediment.65, pp. 1-11.
- Uda, T., Serizawa, M., Miyahara, S., and San-nami, T. 2013. Prediction of segmentation and mergence of shallow water bodies by wind waves using BG model, *Proc. Coastal Dynamics 2013*, Paper No. 166, pp. 1729-1740.
- Wilson, B. W. 1965. Numerical prediction of ocean waves in the North Atlantic for December, 1959, *Deut. Hydrogr. Zeit, Jahrgang 18, Heft 3*, 114-130.
- Zenkovich, V. P. 1967. *Processes of Coastal Development*, Interscience Publishers, New York, 751 p.